Electronic Supplementary Material (ESI) for Dalton Transactions.

^{15}N NMR spectroscopy unambiguously establishes the coordination mode of the diimine linker 2-(2′-pyridyl)pyrimidine-4-carboxylic acid (cppH) in Ru(II) complexes.

Federica Battistin,[a] Gabriele Balducci,[a] Nicola Demitri,[b] Elisabetta Iengo,[a] Barbara Milani,[a]* Enzo Alessio[a]*

[a] Department of Chemical and Pharmaceutical Sciences, University of Trieste, Via L. Giorgieri 1, 34127 Trieste, Italy. Email: alessi@units.it.
[b] Elettra – Sincrotrone Trieste, S.S. 14 Km 163.5 in Area Science Park, 34149 Basovizza – Trieste, Italy.

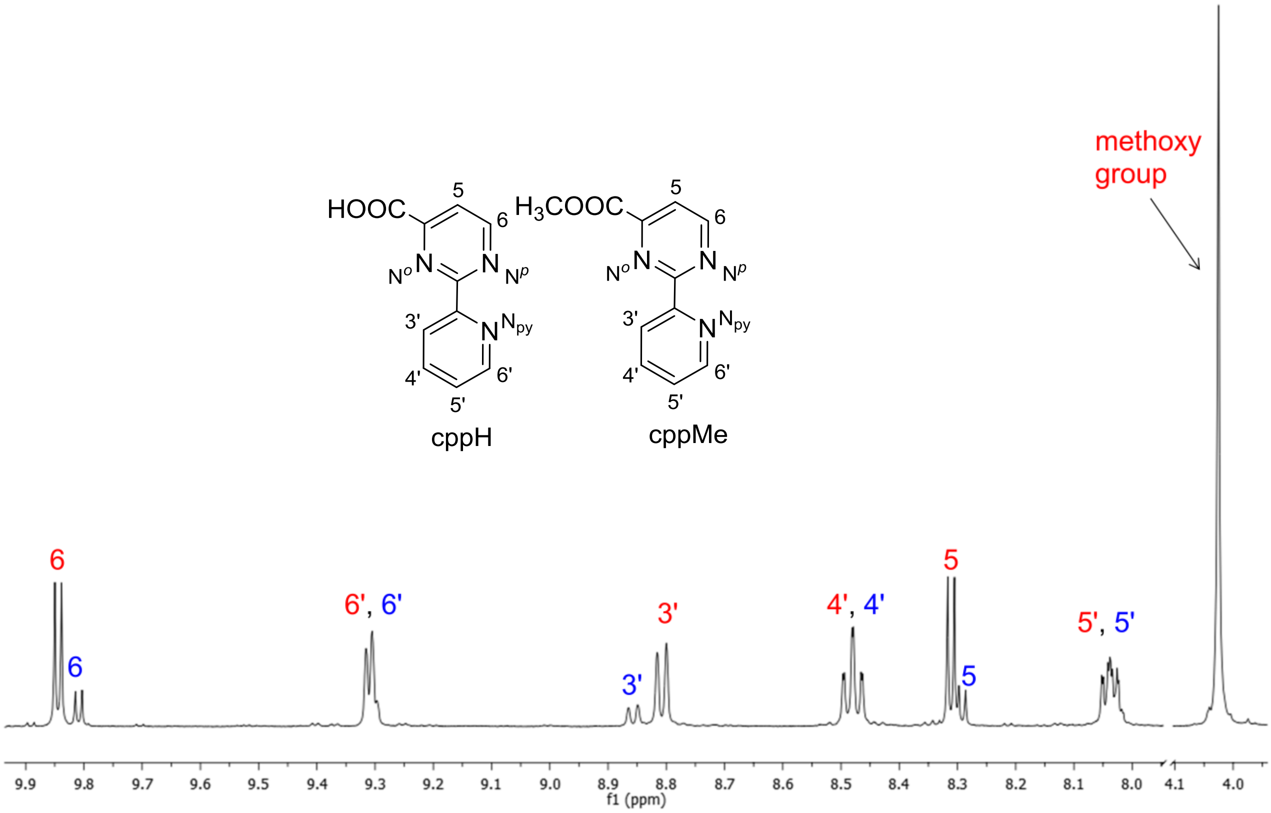

Figure 1S. ^{1}H NMR spectrum of a mixture of *trans,cis*-[RuCl$_2$(CO)$_2$(cppH)] (**5**, blue labels) and *trans,cis*-[RuCl$_2$(CO)$_2$(cppMe)] (**5Me**, red labels) in DMSO-d_6. In the inset, cppH and cppMe with numbering schemes and labels.

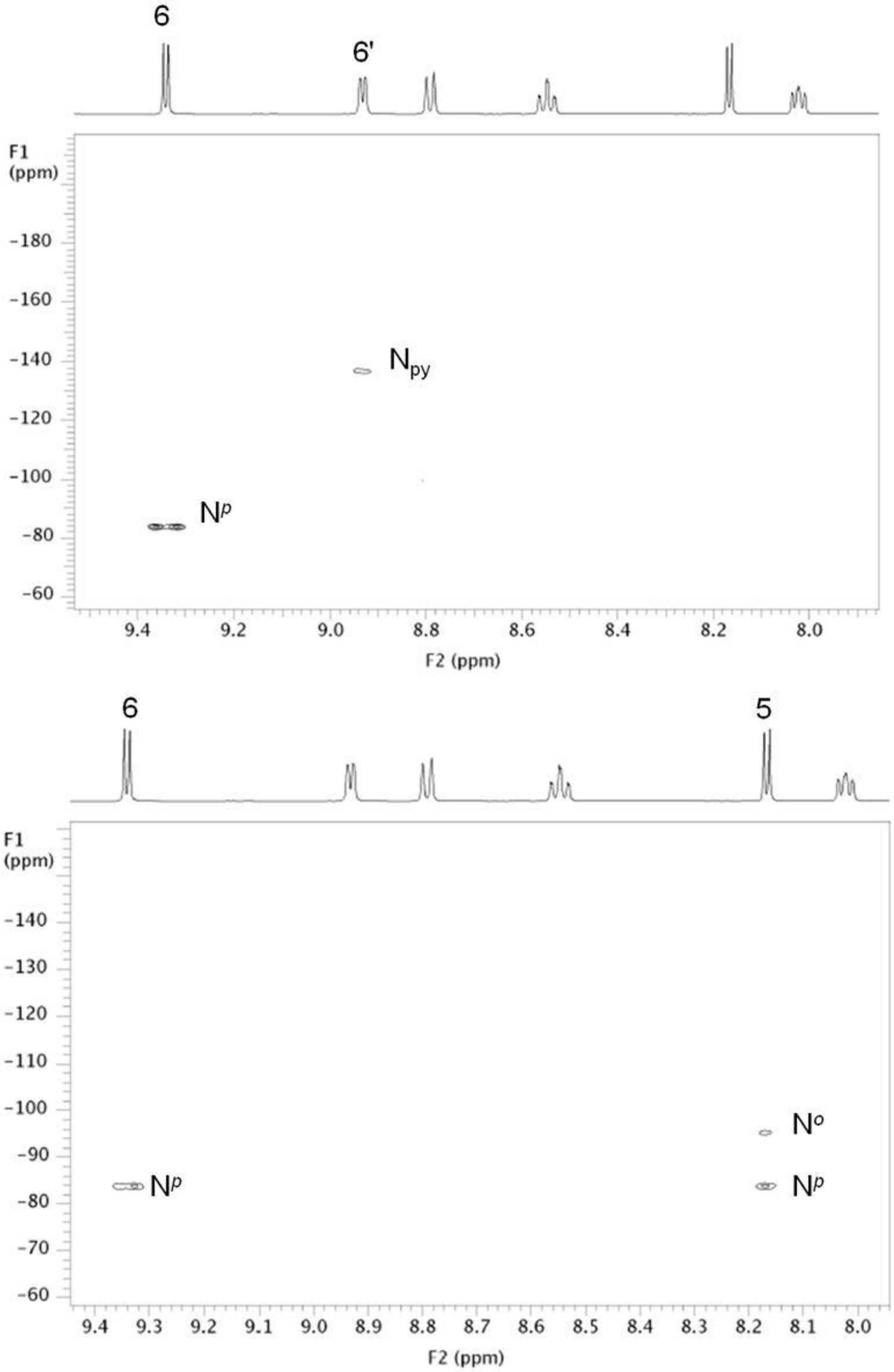

Figure 2S. {^{1}H,^{15}N}- HMBC spectra of cppH·HNO$_3$ in DMSO-*d*$_6$ with *J* = 11 Hz (top) and with *J* = 1.8 Hz (bottom). See the inset of Figure 1S for numbering scheme and labels.

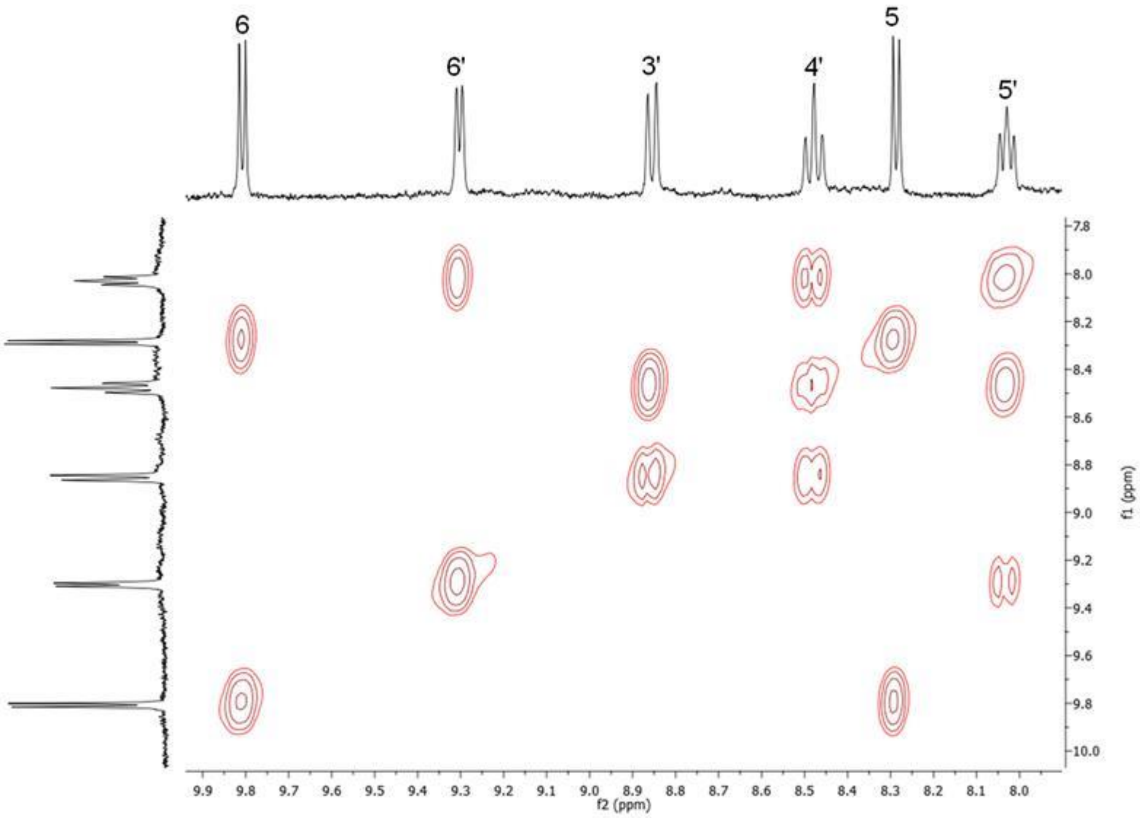

Figure 3S. H-H COSY NMR spectrum of *trans*,*cis*-$[RuCl_2(CO)_2(cppH\text{-}\kappa N^p)]$ (**5**) in DMSO-d_6. See the inset of Figure 1S for numbering scheme.

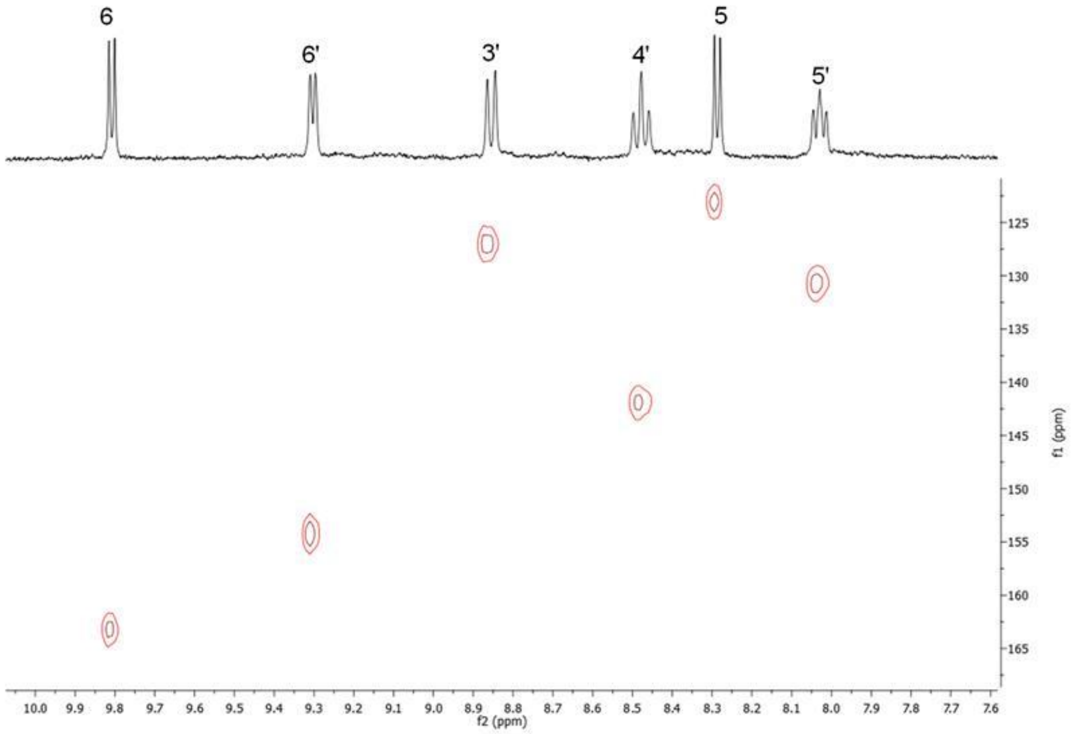

Figure 4S. HSQC NMR spectrum of *trans*,*cis*-$[RuCl_2(CO)_2(cppH\text{-}\kappa N^p)]$ (**5**) in DMSO-d_6. See the inset of Figure 1S for numbering scheme.

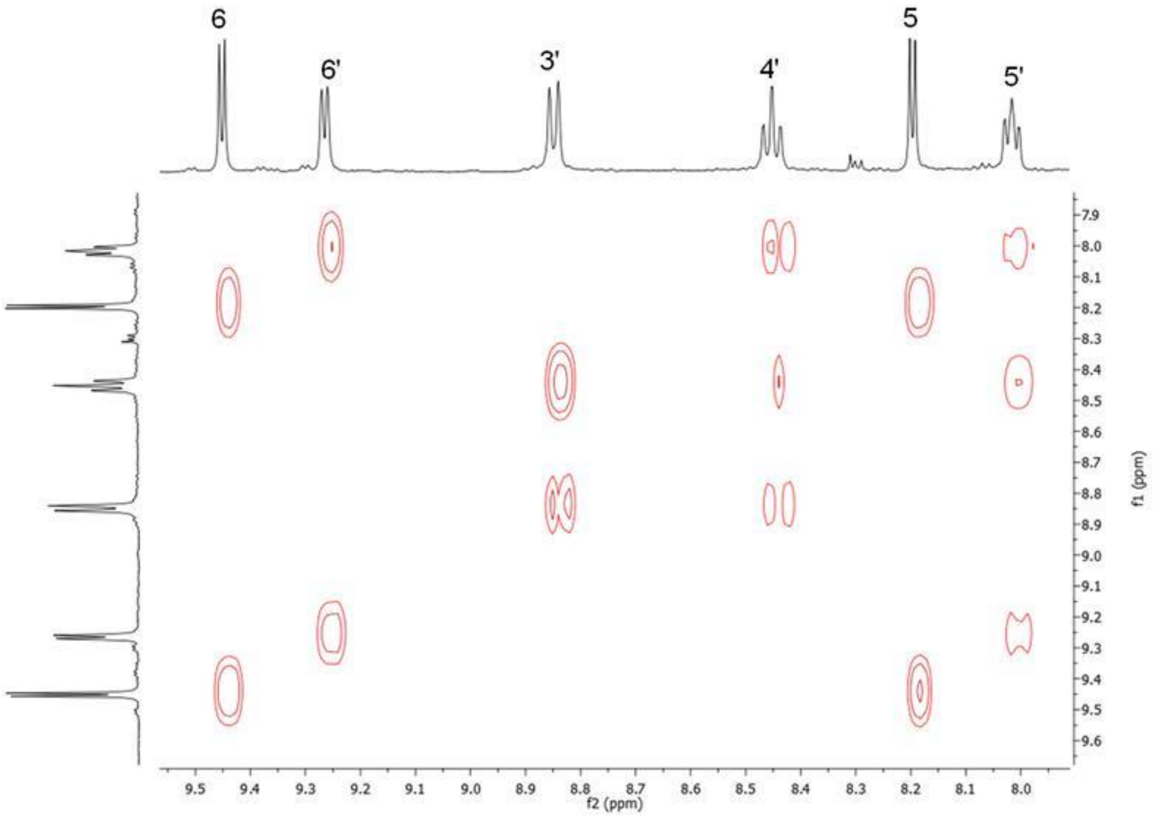

Figure 5S. H-H COSY NMR spectrum of *trans*,*cis*-[RuCl$_2$(CO)$_2$(cppH-κN^p)] (**6**) in DMSO-d_6. See the inset of Figure 1S for numbering scheme.

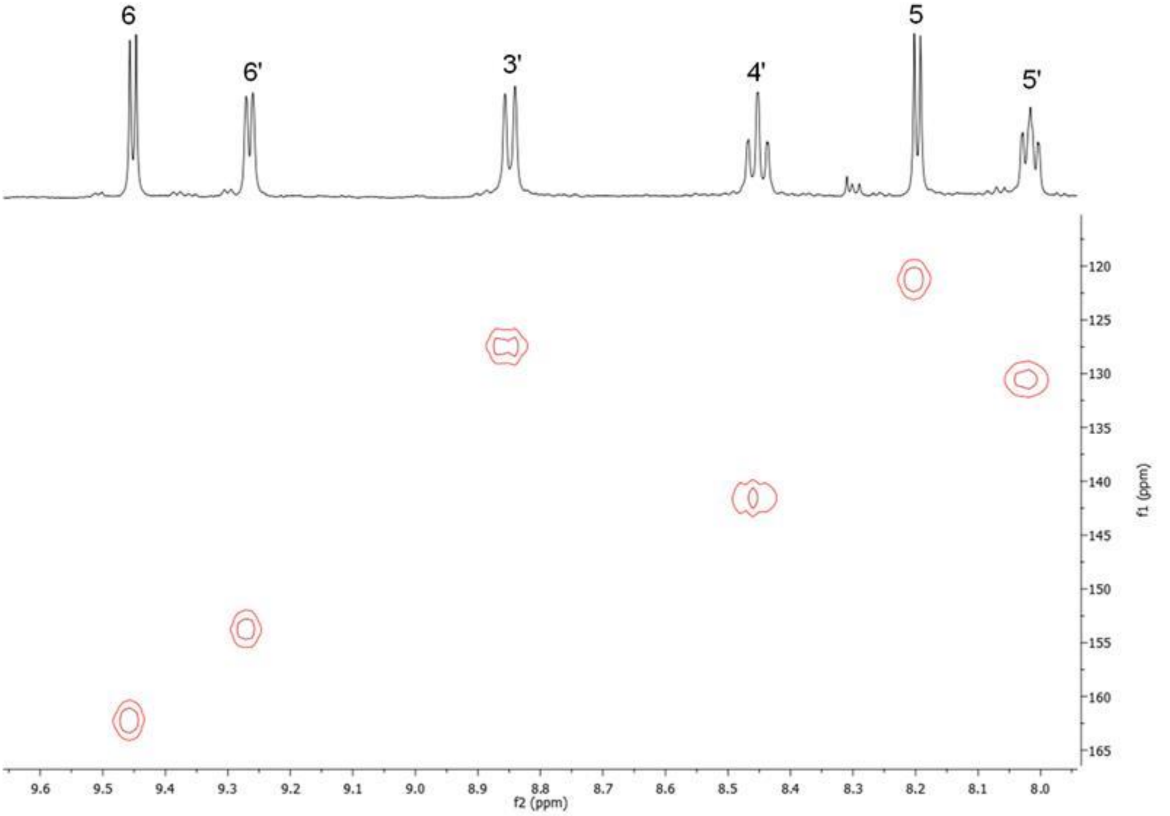

Figure 6S. HSQC NMR spectrum of *trans*,*cis*-[RuCl$_2$(CO)$_2$(cppH-κN^p)] (**6**) in DMSO-d_6. See the inset of Figure 1S for numbering scheme.

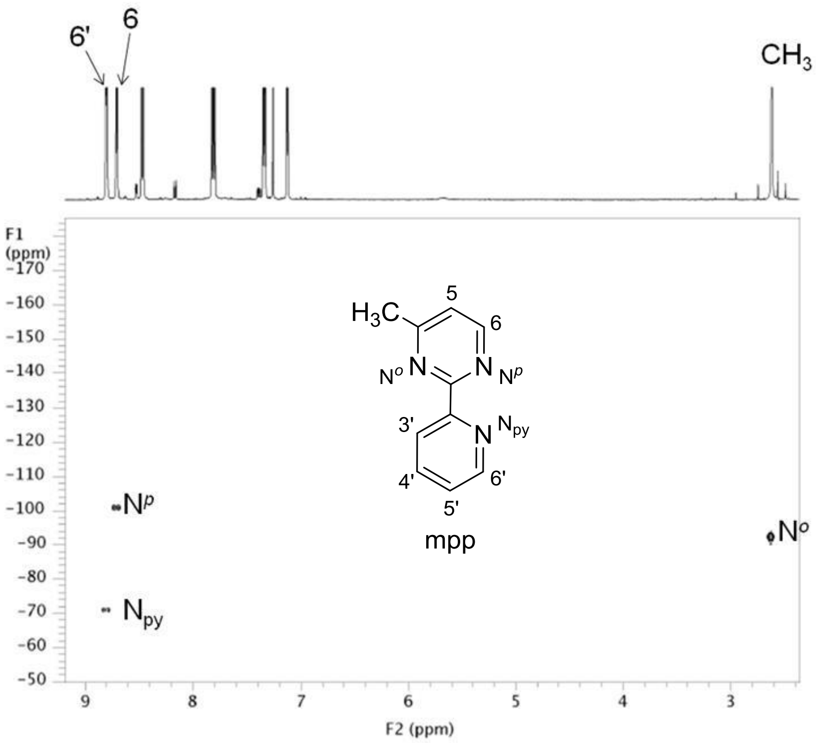

Figure 7S. $\{^1H,^{15}N\}$- HMBC spectrum of mpp with J = 11 Hz in $CDCl_3$. In the inset, mpp with numbering scheme and labels.

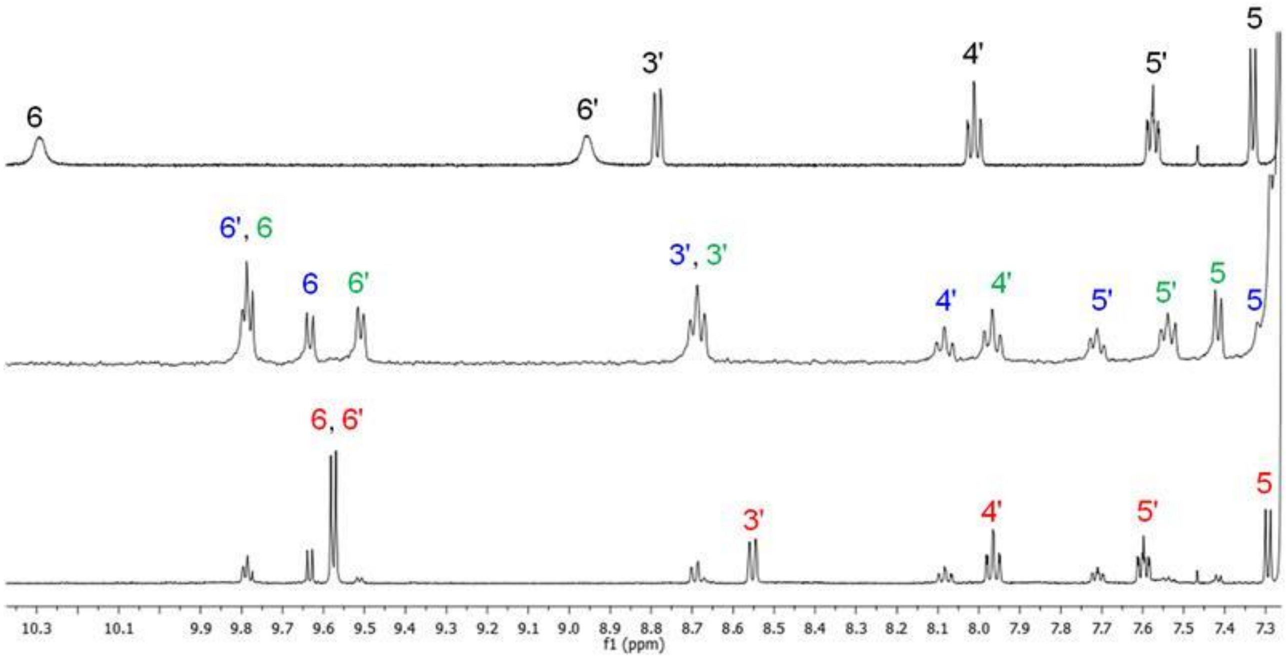

Figure 8S. ^1H NMR spectra (aromatic region) of *cis,trans*-$[RuCl_2(dmso\text{-}S)_2(mpp\text{-}\kappa N^p)]$ (**7**, bottom, with minor amounts of **8** and **9**), a mixture of the two *cis,cis*-$[RuCl_2(dmso\text{-}S)_2(mpp\text{-}\kappa N^p)]$ isomers (**8** + **9**, middle), and *trans,cis*-$[RuCl_2(dmso\text{-}S)_2(mpp\text{-}\kappa N^p)]$ (**10**, top) in $CDCl_3$. See the inset of Figure 7S for numbering scheme.

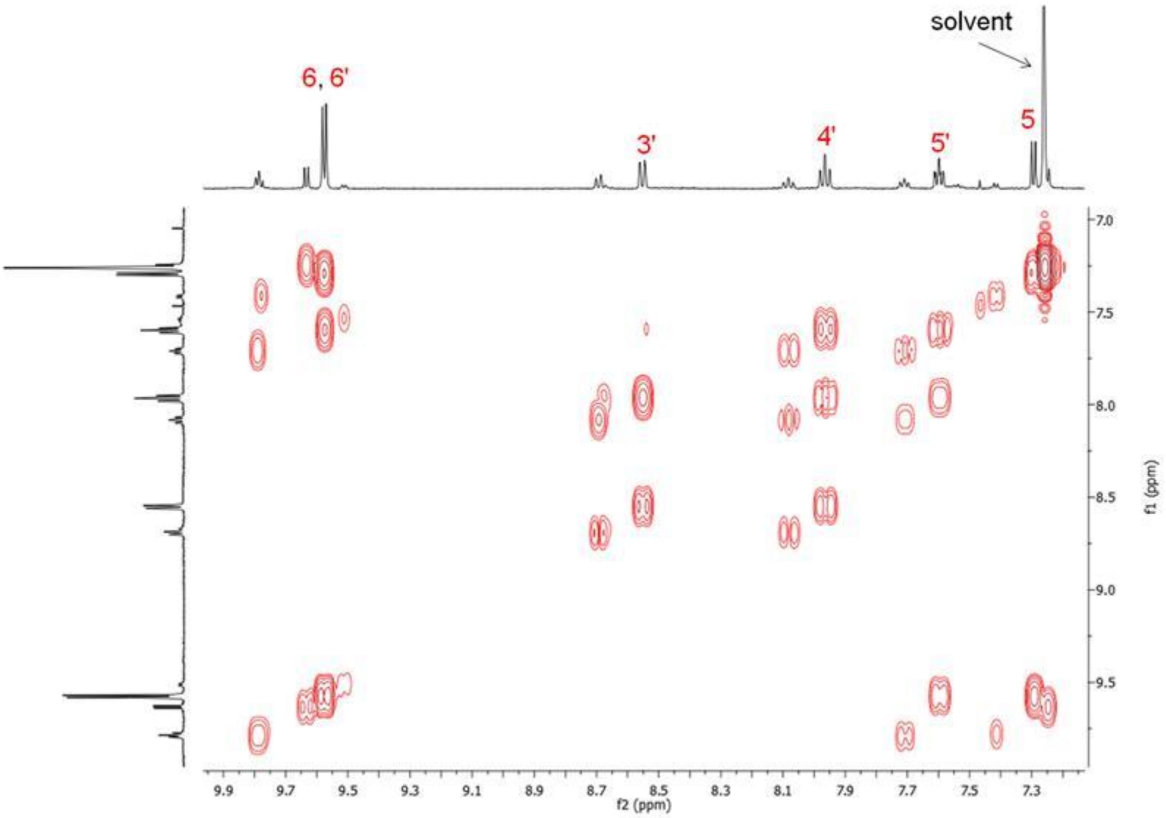

Figure 9S. H-H COSY NMR spectrum (aromatic region) of *cis*,*trans*-[RuCl$_2$(dmso-S)$_2$(mpp-κN^p)] (**7**, with minor amounts of **8** and **9**) in CDCl$_3$. See the inset of Figure 7S for numbering scheme.

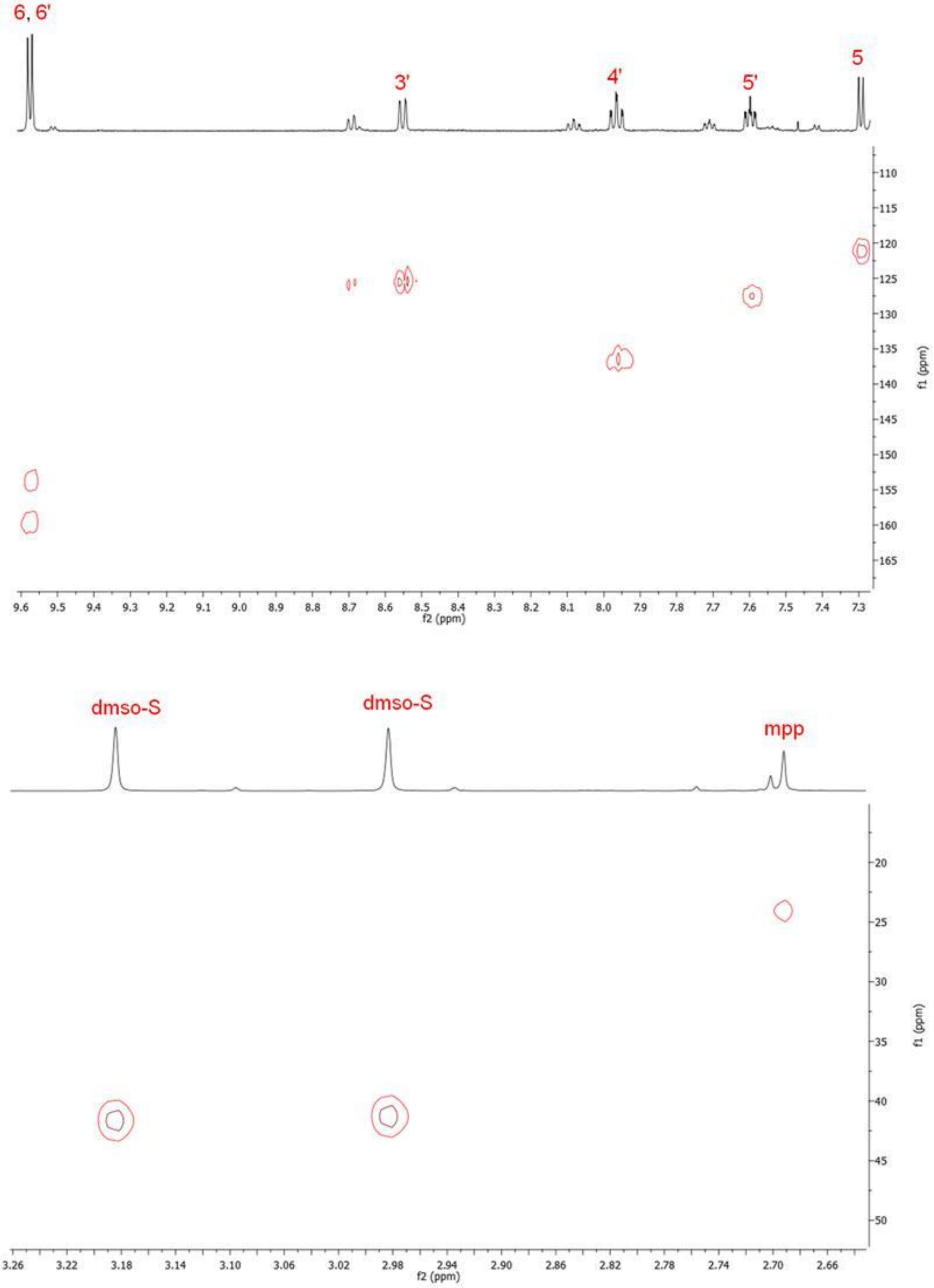

Figure 10S. HSQC NMR spectrum of *cis*,*trans*-[RuCl$_2$(dmso-S)$_2$(mpp-κN^p)] (7, with minor amounts of **8** and **9**) in CDCl$_3$: aromatic region (top) and methyl region (bottom). See the inset of Figure 7S for numbering scheme.

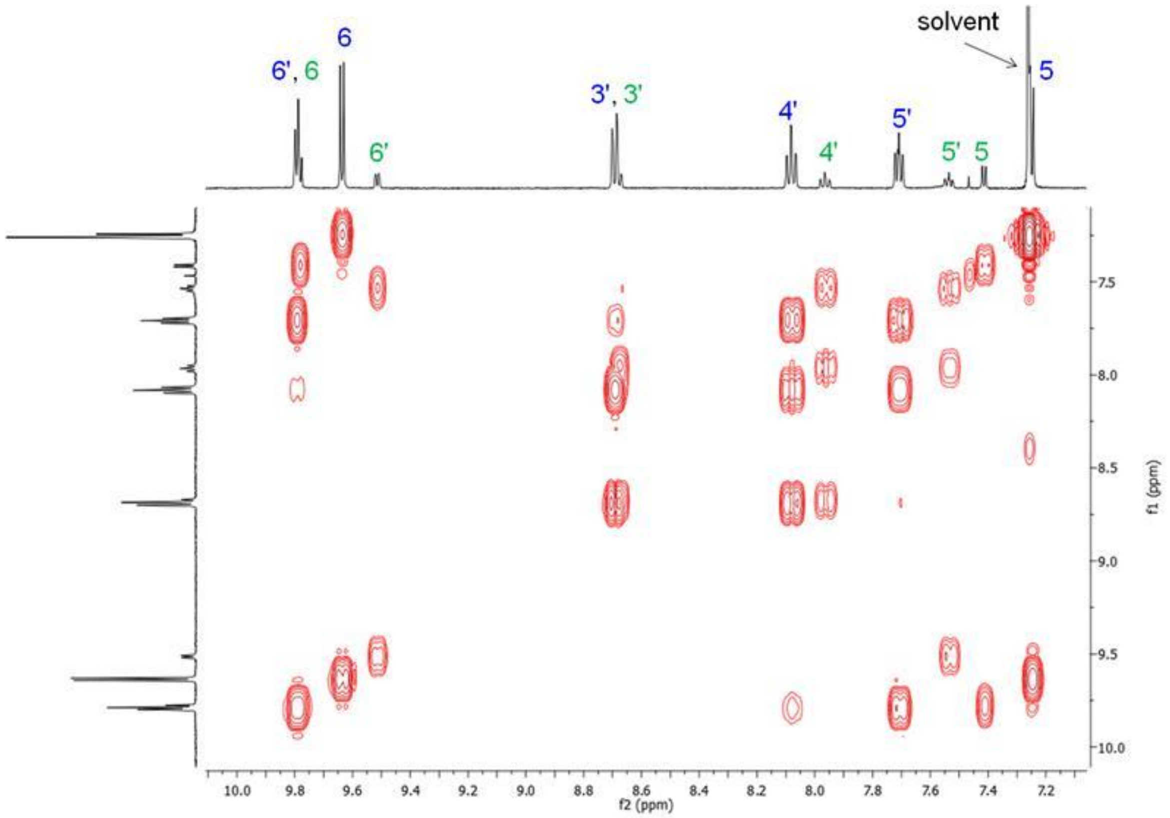

Figure 11S. H-H COSY NMR spectrum (aromatic region) of a mixture of the two *cis,cis*-[$RuCl_2$(dmso-S)$_2$(mpp-κN^p)] isomers (**8** + **9**) in $CDCl_3$. See the inset of Figure 7S for numbering scheme.

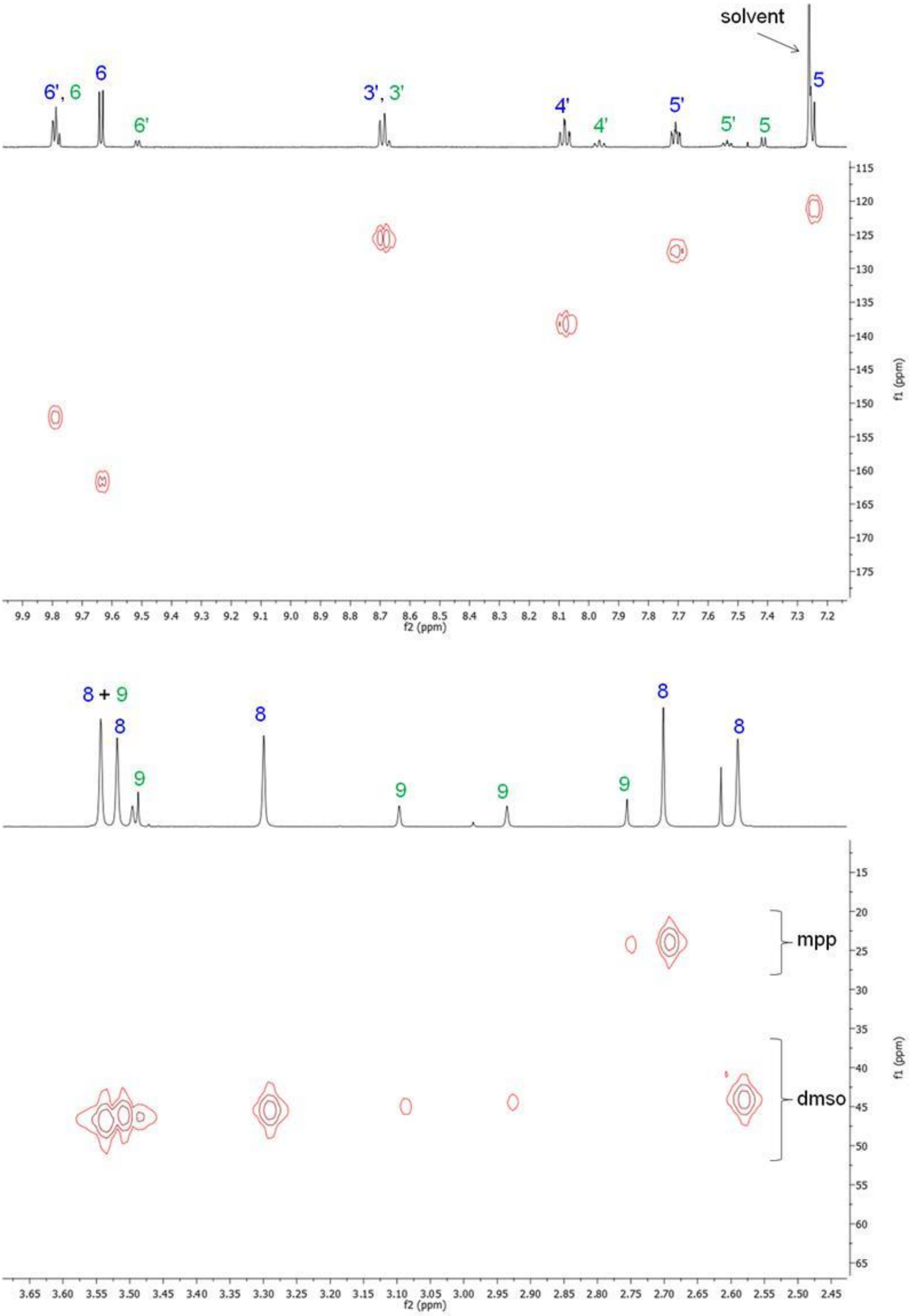

Figure 12S. HSQC NMR spectrum of a mixture of the two *cis*,*cis*-[$RuCl_2$(dmso-S)$_2$(mpp-κN^p)] isomers (**8** + **9**) in $CDCl_3$: aromatic region (top) and methyl region (bottom). See the inset of Figure 7S for numbering scheme.

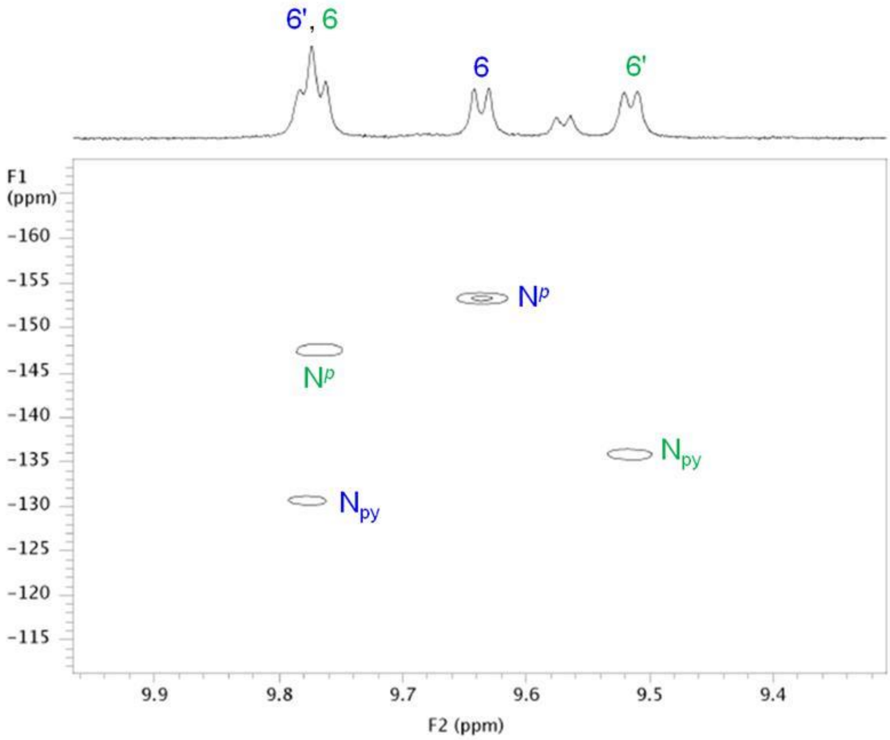

Figure 13S. {^{1}H,^{15}N}- HMBC spectrum (aromatic resonances of mpp) of a mixture of the two *cis,cis*-[RuCl$_2$(dmso-S)$_2$(mpp-κN^p)] isomers (**8** + **9**) with J = 11 Hz in CDCl$_3$. See the inset of Figure 7S for numbering scheme and labels.

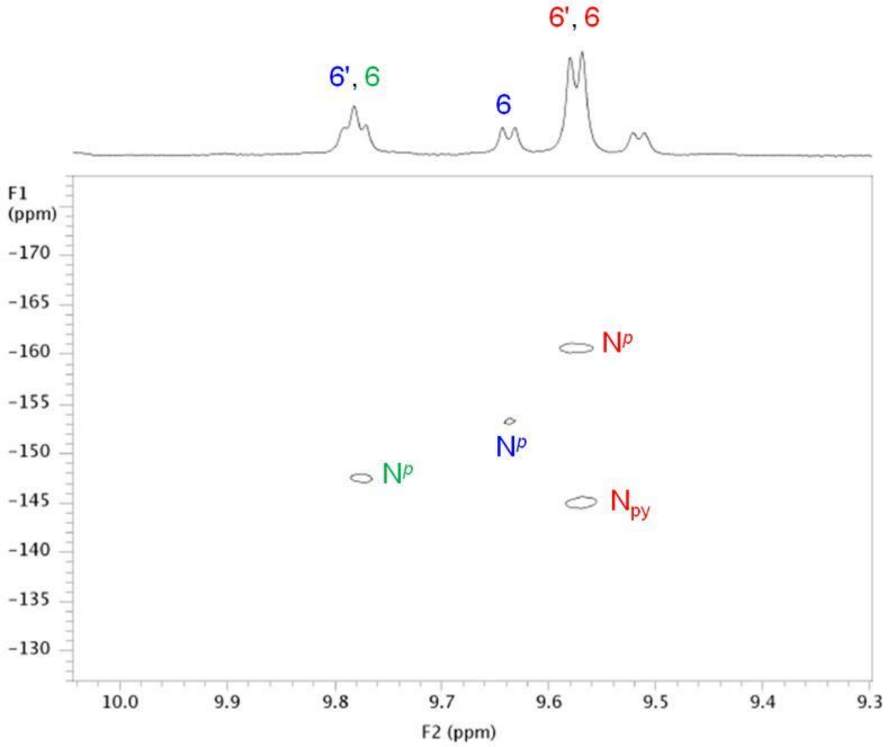

Figure 14S. {^{1}H,^{15}N}- HMBC spectrum (aromatic resonances of mpp) of a mixture of *cis,trans*-[RuCl$_2$(dmso-S)$_2$(mpp-κN^p)] (**7**), and the two *cis,cis*-[RuCl$_2$(dmso-S)$_2$(mpp-κN^p)] isomers (**8** + **9**), with J = 11 Hz in CDCl$_3$. See the inset of Figure 7S for numbering scheme and labels.

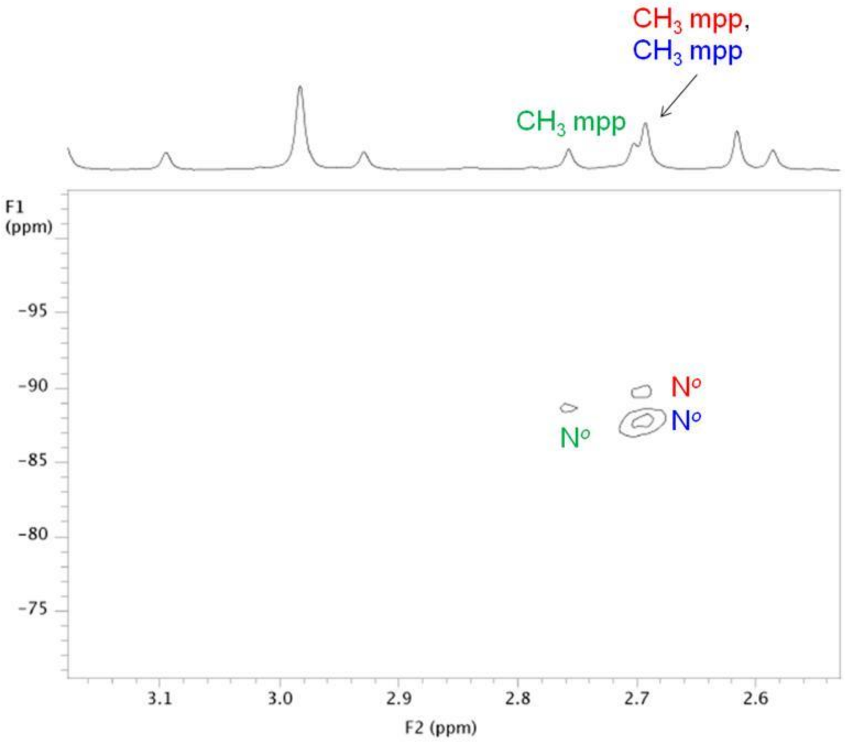

Figure 15S. {^{1}H,^{15}N}- HMBC spectrum (region of methyl resonances) of a mixture of *cis*,*trans*-[RuCl$_2$(dmso-S)$_2$(mpp-κN^p)] (**7**), and the two *cis*,*cis*-[RuCl$_2$(dmso-S)$_2$(mpp-κN^p)] isomers (**8** + **9**), with J = 1.8 Hz in CDCl$_3$. See the inset of Figure 7S for numbering scheme and labels.

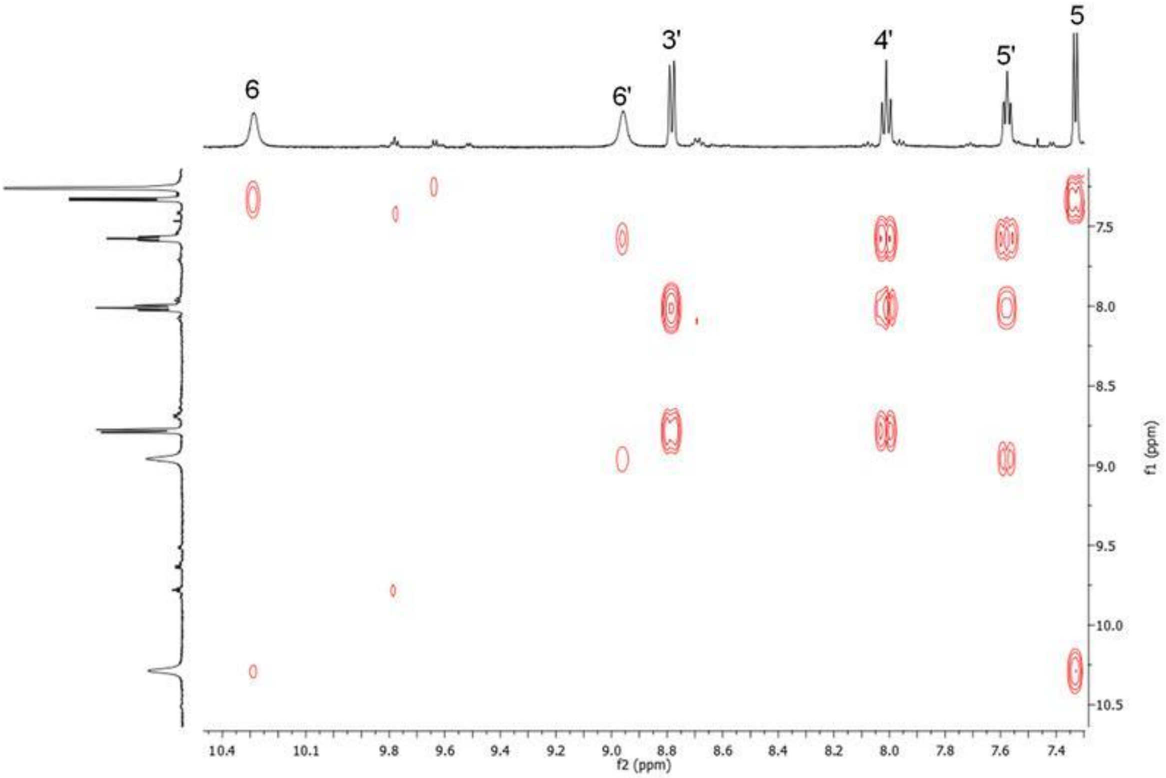

Figure 16S. H-H COSY NMR spectrum (aromatic region) of *trans*,*cis*-[RuCl$_2$(dmso-S)$_2$(mpp-κN^p)] (**10**) in CDCl$_3$. See the inset of Figure 7S for numbering scheme.

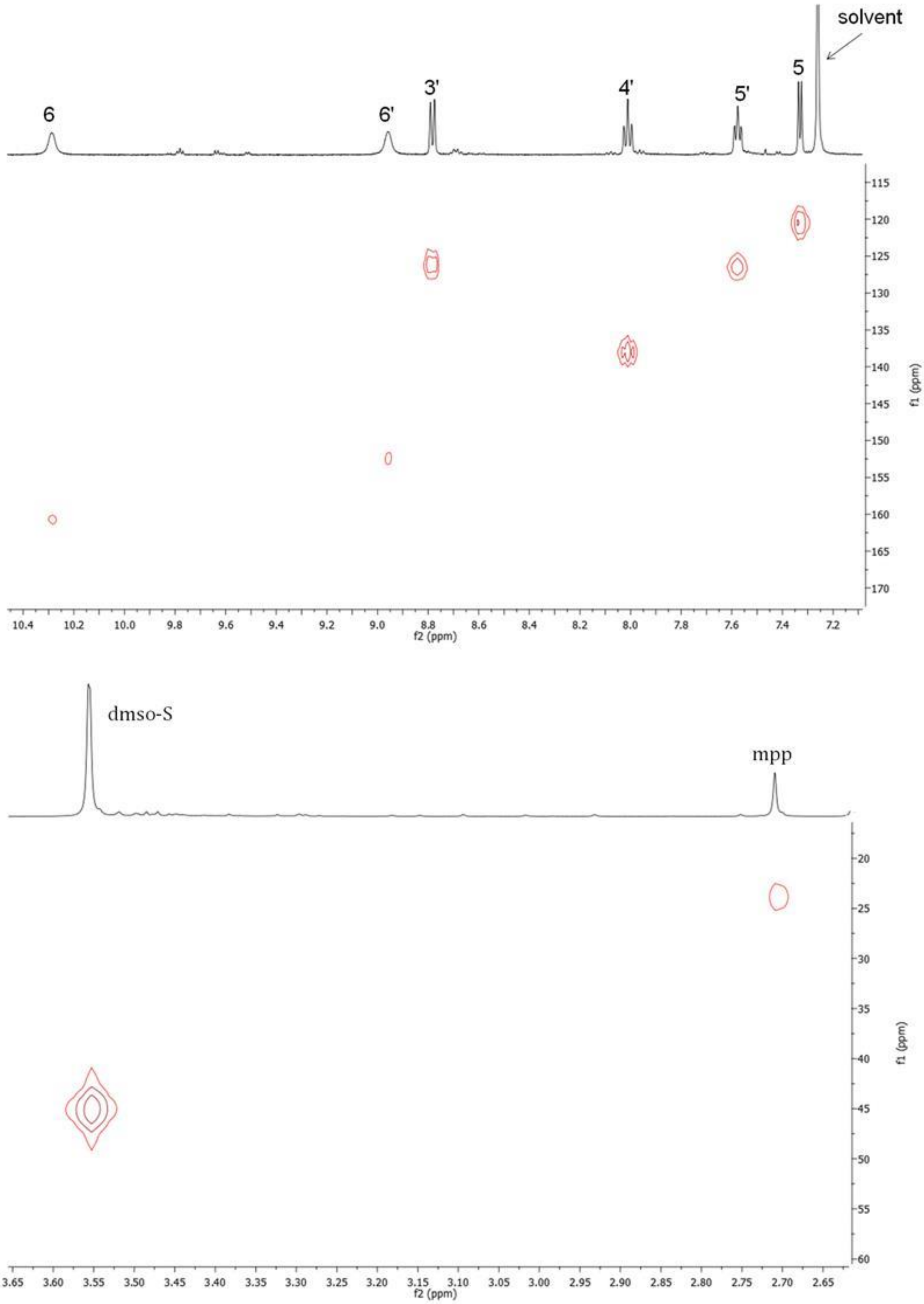

Figure 17S. HSQC NMR spectrum of *trans*,*cis*-[RuCl$_2$(dmso-S)$_2$(mpp-κN^p)] (**10**) in CDCl$_3$: aromatic region (top) and methyl region (bottom). See the inset of Figure 7S for numbering scheme.

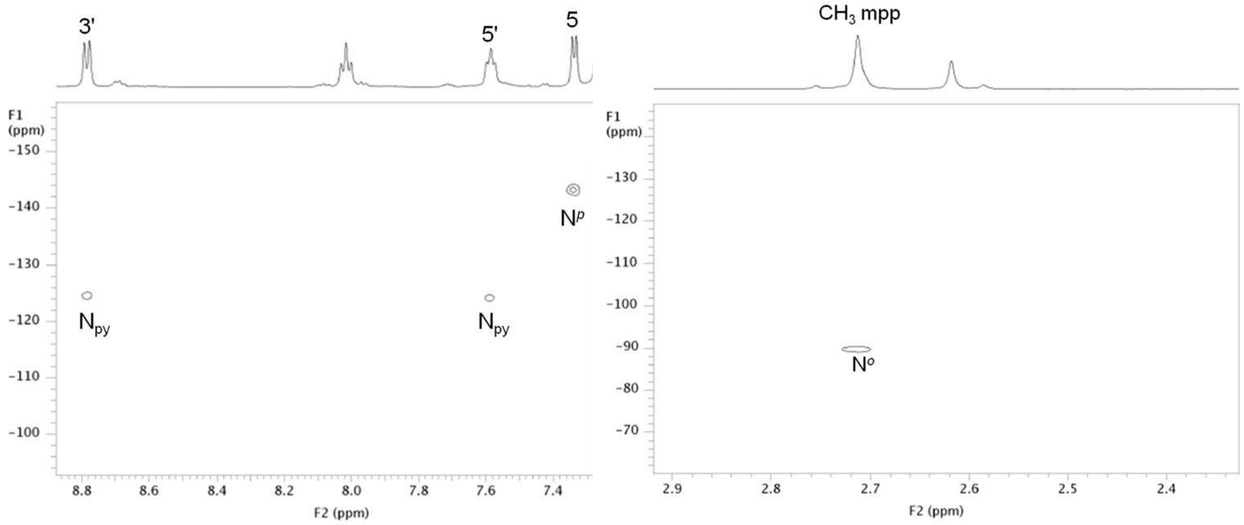

Figure 18S. {^{1}H,^{15}N}- HMBC spectrum of *trans,cis*-[RuCl$_2$(dmso-S)$_2$(mpp-κN^p)] (**10**) with J = 11 Hz in CDCl$_3$. Left: region of the aromatic resonances of mpp; right: region of methyl resonances. See the inset of Figure 7S for numbering scheme and labels.

X-ray structure of 5/5Me

As said in the text, when the preparation of **5** was performed in methanol part of the carboxylate groups of coordinated cppH are methylated and a mixture of *trans,cis*-[RuCl$_2$(CO)$_2$(cppH-κN^p)] (**5**) and *trans,cis*-[RuCl$_2$(CO)$_2$(cppCH$_3$-κN^p)] (**5Me**) cocrystallyzes. The fraction of molecules with esterified cppH has been estimated at 55%. The X-ray structures of **5**, **5Me**, and of the mixture **5**/**5Me** after refinement are shown in Figure 19S.

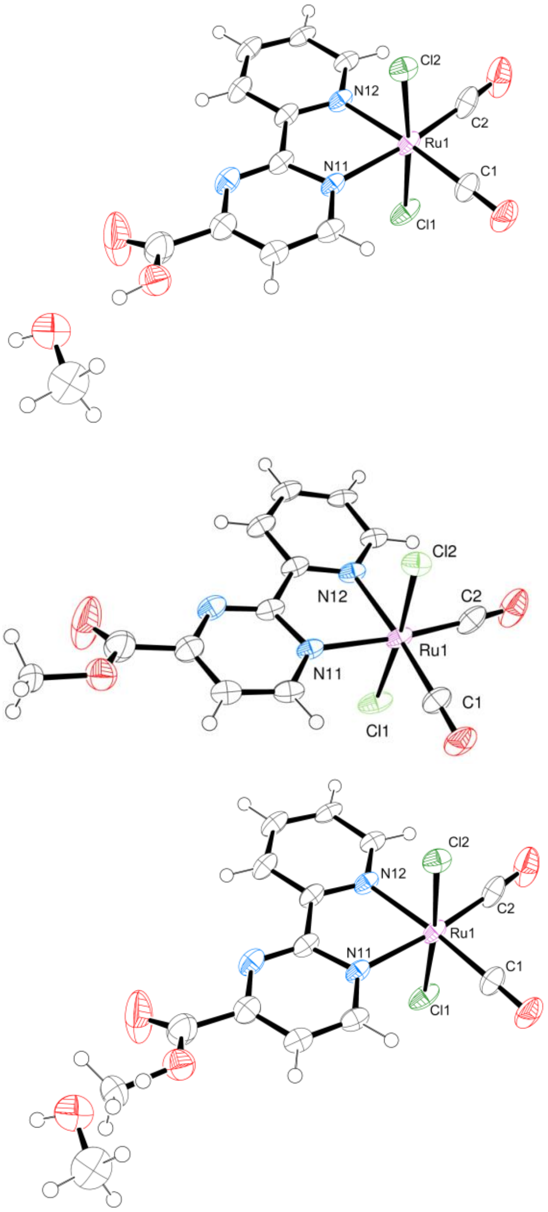

Figure 19S. X-ray structures (50% probability ellipsoids) of *trans,cis*-[RuCl$_2$(CO)$_2$(cppH-κN^p)] (**5**, top), *trans,cis*-[RuCl$_2$(CO)$_2$(cppCH$_3$-κN^p)] (**5Me**, middle), and of the 45/55 mixture **5**/**5Me** (bottom). The fraction of the ASU with a free carboxylic acid moiety shows hydrogen bonding with a methanol molecule.

Crystal packing shows that **5** molecules in **5**/**5Me** crystals are grouped in closely arranged pillars, through π-π stacking interactions. Carboxylate groups are exposed to form channels parallel to unit cell *a* axis, where methanol molecules are coordinated through hydrogen bonds (Figure 20S).

The crystal packings of compounds **7** and **8** show dipole interactions among coordinated dmso-S ligands of neighbor complexes. No solvent molecules were found in these crystals.

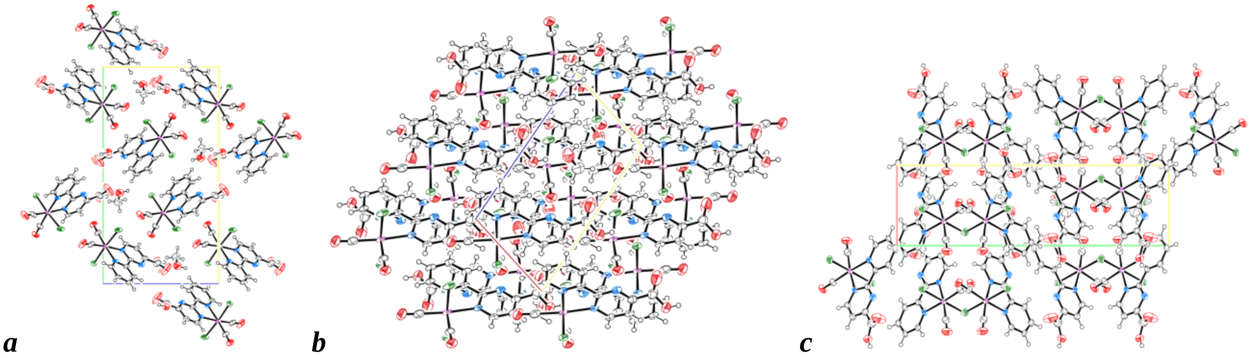

Figure 20S. Crystal packing views of **5**/**5Me** along the crystallographic *a*, *b* and *c* axis, respectively.

Table 1S. Crystallographic data and refinement details for compounds *trans,cis*-[$RuCl_2(CO)_2(cppH\text{-}\kappa N^p)$] + *trans,cis*-[$RuCl_2(CO)_2(cppCH_3\text{-}\kappa N^p)$] (**5**/**5Me**, crystals obtained from MeOH), and *trans,cis*-[$RuCl_2(CO)_2(cppH\text{-}\kappa N^p)$] (**5**, crystals obtained from water).

	5/5Me	**5**
Empirical Formula	$0.45(C_{12}H_7Cl_2N_3O_4Ru)\ 0.45CH_3OH + 0.55(C_{13}H_9Cl_2N_3O_4Ru)$	$C_{12}H_7Cl_2N_3O_4Ru{\cdot}H_2O$
Formula weight (Da)	451.31	447.19
Temperature (K)	100(2)	100(2)
Wavelength (Å)	0.700	0.700
Crystal system	Monoclinic	Monoclinic
Space Group	$P\ 2_1/c$	$P\ 2_1/a$
a (Å)	6.564(1)	13.4180(10)
b (Å)	21.643(4)	8.254(3)
c (Å)	11.766(2)	15.2260(16)
α (°)	90	90
β (°)	103.35(3)	111.383(3)
γ (°)	90	90
V (Å^3)	1626.4(6)	1570.2(5)
Z	4	4
ρ (g·cm^{-3})	1.843	1.892
F(000)	890	880
μ (mm^{-1})	1.247	1.293
θ min,max (°)	1.8, 29.1	1.415, 28.760
Resolution (Å)	0.72	0.73
Total refl. collctd	28444	24489
Independent refl.	4507	4112
Obs. Refl. [Fo>4σ(Fo)]	4264	3689
I/σ(I) (all data)	39.3	21.75
I/σ(I) (max resltn)	25.2	14.24
Completeness (all data)	0.99	0.970
Completeness (max resltn)	0.97	0.962
Rmerge (all data)	0.027	0.053
Rmerge (max resltn,)	0.052	0.091
Multiplicity (all data)	6.0	5.8
Multiplicity (max resltn)	6.1	4.8
Data/restraint/parameters	4507/8/230	4112/3/215
Goof	1.194	1.052
R[I>2.0σ(I)], wR2 [I>2.0σ(I)]	0.0457, 0.1015	0.0428, 0.1182
R (all data), wR2 (all data)	0.0483, 0.1031	0.0475, 0.1239

Table 1S cntd. Crystallographic data and refinement details for compounds *cis,trans*-[RuCl$_2$(dmso-S)$_2$(mpp-κN^p)] (**7**), and *cis,cis*-[RuCl$_2$(dmso-S)$_2$(mpp-κN^p)] (**8**), and *trans,cis*-[RuCl$_2$(dmso-S)$_2$(mpp-κN^p)] (**10**).

	7	**8**	**10**
Empirical Formula	$C_{14}H_{21}Cl_2N_3O_2RuS_2$	$C_{14}H_{21}Cl_2N_3O_2RuS_2$	$C_{14}H_{21}Cl_2N_3O_2RuS_2\cdot 1/3CH_3OH$
Formula weight (Da)	499.43	499.43	510.11
Temperature (K)	100(2)	100(2)	100(2)
Wavelength (Å)	0.700	0.700	0.700
Crystal system	Triclinic	Monoclinic	Trigonal
Space Group	$P\,-1$	$P\,2_1/c$	$R\,-3$
a (Å)	8.275(2)	13.0180(4)	23.0660(14)
b (Å)	9.618(2)	8.2120(8)	23.0660(14)
c (Å)	12.681(3)	17.5210(4)	19.425(4)
α (°)	82.67(3)	90	90
β (°)	73.04(3)	91.93(2)	90
γ (°)	78.60(3)	90	120
V (Å^3)	943.7(4)	1872.0(2)	8950(2)
Z	2	4	18
ρ (g·cm^{-3})	1.758	1.772	1.704
F(000)	504	1008	4644
μ (mm^{-1})	1.275	1.285	1.225
θ min,max (°)	2.1, 30.0	2.9, 31.0	1.440, 28.184
Resolution (Å)	0.70	0.68	0.74
Total refl. collctd	51595	23331	48116
Independent refl.	5690	6013	4993
Obs. Refl. [Fo>4σ(Fo)]	5387	5677	4846
I/σ(I) (all data)	27.6	28.7	59.25
I/σ(I) (max resltn)	14.5	20.3	43.60
Completeness (all data)	1.00	0.97	0.973
Completeness (max resltn)	1.00	0.86	0.977
Rmerge (all data)	0.037	0.033	0.028
Rmerge (max resltn,)	0.067	0.038	0.036
Multiplicity (all data)	4.4	3.9	9.7
Multiplicity (max resltn)	3.2	3.1	9.1
Data/restraint/parameters	5690/0/224	6013/0/222	4993/11/242
Goof	1.138	1.058	1.246
R[I>2.0σ(I)], wR2 [I>2.0σ(I)]	0.0364, 0.0779	0.0247, 0.0619	0.0367, 0.1289
R (all data), wR2 (all data)	0.0386, 0.0789	0.0263, 0.0629	0.0373, 0.1298

Table 2S. Selected coordination distances (Å) and angles (°) for *trans,cis*-[RuCl$_2$(CO)$_2$(cppH-κN^p)] (**5**).

Bond distances (Å)			
Ru1–N1	2.112(2)	Ru1–C1	1.891(3)
Ru1–N2	2.103(2)	Ru1–C2	1.900(3)
Ru1–Cl1	2.3819(7)	Ru1–Cl2	2.4010(7)
Bond angles (°)			
N1–Ru1–N2	77.68(8)	N2–Ru1–Cl2	88.09(6)
N1–Ru1–Cl1	85.30(6)	Cl1–Ru1–C1	91.71(9)
N1–Ru1–C1	99.63(11)	Cl1–Ru1–C2	93.21(9)
N1–Ru1–C2	173.84(10)	Cl1–Ru1–Cl2	171.22(2)
N1–Ru1–Cl2	87.11(6)	C1–Ru1–C2	86.37(13)
N2–Ru1–Cl1	85.98(6)	C1–Ru1–Cl2	93.91(9)
N2–Ru1–C1	176.57(10)	C2–Ru1–Cl2	93.88(9)
N2–Ru1–C2	96.27(10)		

Table 3S. Selected coordination distances (Å) and angles (°) for *trans,cis*-[RuCl$_2$(CO)$_2$(cppCH$_3$-κN^p)] (**5Me**).

Bond distances (Å)			
Ru1–N11	2.124(3)	Ru1–C2	1.880(5)
Ru1–N12	2.113(3)	Ru1–C1	1.874(4)
Ru1–Cl2	2.396(1)	Ru1–Cl1	2.388(1)
Bond angles (°)			
N11–Ru1–N12	77.4(1)	N12–Ru1–Cl1	88.76(9)
N11–Ru1–Cl2	87.50(8)	Cl2–Ru1–C2	92.2(1)
N11–Ru1–C2	172.8(1)	Cl2–Ru1–C1	91.8(1)
N11–Ru1–C1	97.3(2)	Cl2–Ru1–Cl1	175.18(4)
N11–Ru1–Cl1	88.24(8)	C2–Ru1–C1	89.9(2)
N12–Ru1–Cl2	88.10(9)	C2–Ru1–Cl1	91.8(2)
N12–Ru1–C2	95.4(2)	C1–Ru1–Cl1	91.0(1)
N12–Ru1–C1	174.7(2)		

Table 4S. Selected coordination distances (Å) and angles (°) for *cis*,*trans*-[$RuCl_2$(dmso-S)$_2$(mpp-κN^p)] (**7**).

Bond distances (Å)			
Ru1–N11	2.057(2)	Ru1–Cl1	2.426(1)
Ru1–N12	2.056(3)	Ru1–Cl2	2.427(1)
Ru1–S1	2.2981(9)	Ru1–S2	2.2977(9)
Bond angles (°)			
N11–Ru1–N12	79.03(9)	N12–Ru1–S2	89.10(7)
N11–Ru1–S1	91.75(6)	S1–Ru1–Cl1	89.16(3)
N11–Ru1–Cl1	173.46(6)	S1–Ru1–Cl2	89.01(3)
N11–Ru1–Cl2	94.21(6)	S1–Ru1–S2	177.71(3)
N11–Ru1–S2	89.47(6)	Cl1–Ru1–Cl2	92.28(3)
N12–Ru1–S1	93.04(7)	Cl1–Ru1–S2	89.85(3)
N12–Ru1–Cl1	94.45(7)	Cl2–Ru1–S2	88.97(2)
N12–Ru1–Cl2	172.99(7)		

Table 5S. Selected coordination distances (Å) and angles (°) for *cis*,*cis*-[RuCl$_2$(dmso-S)$_2$(mpp-κN^p)] (**8**).

Bond distances (Å)			
Ru1–N11	2.0525(12)	Ru1–Cl2	2.4193(4)
Ru1–N12	2.1025(12)	Ru1–S1	2.2742(4)
Ru1–Cl1	2.4396(4)	Ru1–S2	2.2441(4)
Bond angles (°)			
N11–Ru1–N12	78.11(5)	N12–Ru1–S2	93.51(4)
N11–Ru1–Cl1	87.61(4)	Cl1–Ru1–Cl2	92.84(1)
N11–Ru1–Cl2	170.83(3)	Cl1–Ru1–S1	87.67(2)
N11–Ru1–S1	98.64(4)	Cl1–Ru1–S2	176.52(1)
N11–Ru1–S2	90.02(4)	Cl2–Ru1–S1	90.53(2)
N12–Ru1–Cl1	83.52(4)	Cl2–Ru1–S2	89.10(2)
N12–Ru1–Cl2	92.83(4)	S1–Ru1–S2	95.20(2)
N12–Ru1–S1	170.71(4)		

Table 6S. Selected coordination distances (Å) and angles (°) for *trans,cis*-[RuCl$_2$(dmso-S)$_2$(mpp-κN^p)] (**10**).

Bond distances (Å)			
Ru1–N31	2.1344(17)	Ru1–Cl2	2.3924(6)
Ru1–N32	2.1246(16)	Ru1–S1	2.3002(5)
Ru1–Cl1	2.3829(6)	Ru1–S2	2.2646(5)
Bond angles (°)			
N31–Ru1–N32	76.52(7)	N32–Ru1–S2	97.74(5)
N31–Ru1–Cl1	89.91(5)	Cl1–Ru1–Cl2	176.075(18)
N31–Ru1–Cl2	87.43(5)	Cl1–Ru1–S2	92.96(2)
N31–Ru1–S1	95.66(5)	Cl1–Ru1–S1	91.712(18)
N31–Ru1–S2	173.44(5)	Cl2–Ru1–S2	89.40(2)
N32–Ru1–Cl1	86.64(4)	Cl2–Ru1–S1	91.421(18)
N32–Ru1–Cl2	89.94(4)	S1–Ru1–S2	90.161(19)
N32–Ru1–S1	172.00(5)		